ACS APPLIED MATERIALS & INTERFACES

Research Article

www.acsami.org

In Vitro Evaluation of the Tribological Response of Mo-Doped Graphite-like Carbon Film in Different Biological Media

Jinxia Huang,[†,‡] Liping Wang,*[,†] Bin Liu,[§] Shanhong Wan,[†] and Qunji Xue[†]

[†]State Key Laboratory of Solid Lubrication, Lanzhou Institute of Chemical Physics, Chinese Academy of Sciences, Lanzhou, 730000, P. R. China

[‡]University of Chinese Academy of Sciences, Beijing100039, P. R. China

[§]School of Stomatology, Lanzhou University, Lanzhou, 730000, P. R. China

ABSTRACT: Complicated tribochemical reactions with the surrounding media often occur at the prosthesis material, which is a dominant factor causing the premature failure in revision surgery. Graphite-like carbon (GLC) film has been proven to be an excellent tribological adaption to water-based media, and this work focused on the friction and wear behavior of Mo-doped GLC (Mo-GLC)-coated poly(aryl ether ether ketone) sliding against Al_2O_3 counterpart in physiological saline, simulated body fluid, and fetal bovine serum (FBS), which mainly emphasized the interface interactions of the prosthetic materials/lubricant. Results showed different tribological responses of Mo-GLC/Al_2O_3 pairs strongly correlated with the interfacial reactions of the contacting area. Particularly, a transfer layer was believed to be responsible for the excellent wear reduction of Mo-GLC/Al_2O_3 pair in FBS medium, in which graphitic carbon and protein species were contained. The wear mechanisms are tentatively discussed according to the morphologies and chemical compositions of the worn surfaces examined by scanning electron microscope as well as X-ray photoelectron spectroscopy.

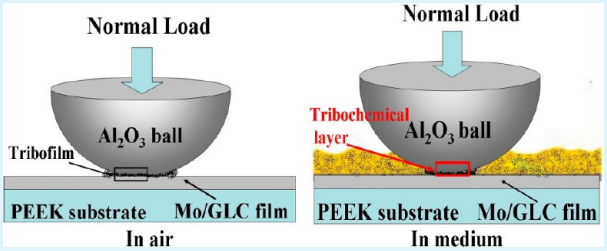

KEYWORDS: *friction and wear, interfacial interactions, PEEK, graphite-like carbon, biological medium*

1. INTRODUCTION

In the field of prosthetic materials, the improvement of antiwear and antifriction performance of the prosthetic materials interface is imperative for long-term lubricated pairings in the human body.[1] Poly(aryl ether ether ketone) (PEEK), one polymer substituting for metal alloy in joint replacement, shows a desirable combination of high strength, stiffness, and fatigue and wear resistance,[2] as well as being nontoxic and naturally radiolucent.[3] However, PEEK debris inevitably produced due to wear during the sliding process has been earlier proven to induce aseptic loss and osteolysis, causing a failure of total joint replacement.[4,5] Graphite-like carbon (GLC) films have shown excellent tribological adaption in water or humid environments, attaining a combination of highly desirable properties in the context of biomedical applications, as compared to diamond-like carbon (DLC).[6−8]

It is well-known that synovial fluid serves as the lubricant at the articulating joints, and interactions at the interface of the prosthetic materials/synovial fluid inevitably occur under physiological loading conditions, where the synovial fluid has a pH value of 7.4 and a temperature of 37 °C (98.6 °F).[9] However, the wear process in the human body is complicated. Since human body fluids contains both inorganic species and organic giant molecules (i.e., serum proteins), these constituents are entrained into the contact zone during joint movement, which in turn affects the friction and wear response of the prosthetic materials via chemical and mechanical interactions.[10] In particular, tribochemical reactions between the articulating surfaces can damage the biological media and surrounding tissue around the prosthetic materials and lead to the bone loosening.[11,12] Therefore, the tribological performance and service life of the GLC-coated medical devices can be greatly improved by suitable lubrication.[13]

Recent in vitro biotribological studies have shown that NaCl solution,[14] simulated body fluid,[15] bovine serum[16] and model or synthetic fluids[17−19] normally functioned as a biological media, providing low-wear and low-friction properties for the prosthetic joint materials. Among them serum is the most popular lubricant in the wear evaluation of prosthetic joints and their relevant materials because its composition is close to that of the original synovial fluid. However, very few studies have been directly reported about the influence of proteins on the tribological behavior of Mo-doped GLC (Mo-GLC) films and the changes in protein structure after a friction test, which is very important for biomedical materials applications. For example, when in contact with the fetal bovine serum solution, the protein will first adsorb to the surface of the prosthetic materials, which will obviously influence the tribological behavior of GLC films. On the contrary, the thermal and

Received: November 11, 2014
Accepted: December 26, 2014
Published: January 12, 2015

DOI: 10.1021/am507850r
ACS Appl. Mater. Interfaces 2015, 7, 2772−2783

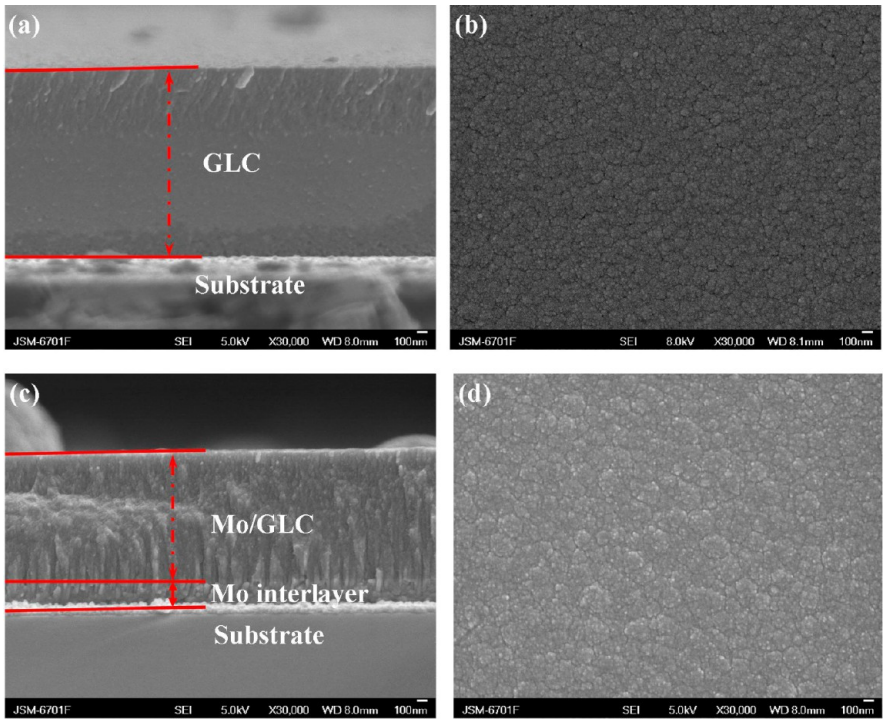

Figure 1. Cross-sectional and surface images of as-fabricated coatings for (a, b) GLC and (c, d) Mo-GLC films.

mechanical action of friction will also affect the microstructural changes of the protein adsorbed on the prosthetic surface.[20]

In this work, metallic Mo is selected as the dopant to modify the GLC surface owing to its high biocompatibility.[21−23] Mo-GLC films were first deposited onto PEEK substrates and the tribological characteristic of Mo-GLC-coated PEEK sliding against Al_2O_3 were systemically investigated in different biological lubricants. For comparison, the tribological properties of the GLC films under dry conditions are examined as well. In order to fully optimize the tribological behavior of carbon-based films for biomedical applications, the worn surfaces of the Mo-GLC/Al_2O_3 pairing were analyzed as well as the interfacial reactions at the rubbing surface.

2. EXPERIMENTAL SECTION

2.1. Sample Preparation. The specimens, with a dimension of Φ 25 × 3 mm^2, were cut from a bulk semicrystalline PEEK rod. These cut specimens were first diamond-polished until a final surface roughness of R_a = 140 nm as determined by a surface profilometer. Prior to deposition, the PEEK substrates were ultrasonically cleaned in acetone and alcohol baths in succession for 15 min and dried with a blower. The GLC films were deposited on PEEK substrates by an unbalanced magnetron sputtering technique in a multitarget PVD system. A graphite target (purity 99.95%) with dimensions of 6 × 76 × 153 mm^3 for sputtering carbon was used. A base pressure of 2.0 × 10^{-3} Pa in the chamber was attained with a turbomolecular pumping system, and then the total pressure was set at a pressure of 0.6 Pa by Ar inflation with a flow rate of 120 sccm. As the pressure of the vacuum chamber was reached, PEEK substrates were sputter cleaned in situ for 15 min in argon plasma at a dc bias voltage of −1000 V and a duty cycle of 50%. Meanwhile, the rotation speed of PEEK substrate was 5 rpm during the depositing process. Finally, GLC film was deposited at a dc current of 1.2A and a bias voltage of −300 V. The total deposition process lasted for 100 min.

As ref 13 reported, Mo-GLC film was deposited onto PEEK substrates, as well as pure GLC film. GLC film had a thickness of around 1700 nm and showed a uniformly smooth surface finish consisting of nanometer-sized particles, as shown in in Figure 1a. As for Mo-GLC composite film, its total thickness is around 1400 nm, where the Mo intermediate layer accounted for 200 nm, as shown in Figure 1c. In contrast with GLC film, Mo-GLC film grew with a homogeneously glassy columnar feature, as seen in the cross-sectional SEM image. It was also found that the columnar microstructure would disappear on the surface of the Mo-GLC film when the Mo content decreased to a low range. Furthermore, GLC and Mo-GLC film has a higher I_D/I_G ratio of ∼3.24 and ∼3.58, respectively, well consistent with graphite-like amorphous structure according to the Gaussian-fitted Raman spectrum (Figure 2).[24,25]

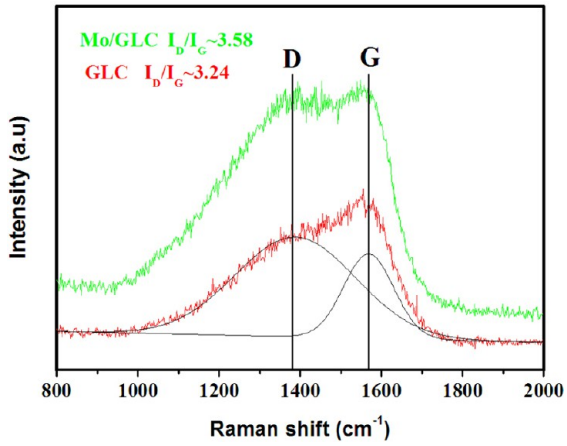

Figure 2. Gaussian−Lorentzian fitted Raman spectrum of GLC and Mo-GLC films.

Full-scale XPS spectra of Mo-GLC give a composition of 6.69 atom % Mo and 12.36 atom % O with a carbon content 80.95 atom %, respectively (Figure 3), while GLC film is made up of 82.78 atom % C and 17.22 atom % O. As compared with the C 1s line of the GLC film, a band lies at 283.0 eV, which indicates the existence of carbide species,[26] and the Mo 3d line having a band at 228.5 eV also confirms that Mo bonds with carbon during the depositing process.[27,28]

DOI: 10.1021/am507850r
ACS Appl. Mater. Interfaces 2015, 7, 2772−2783

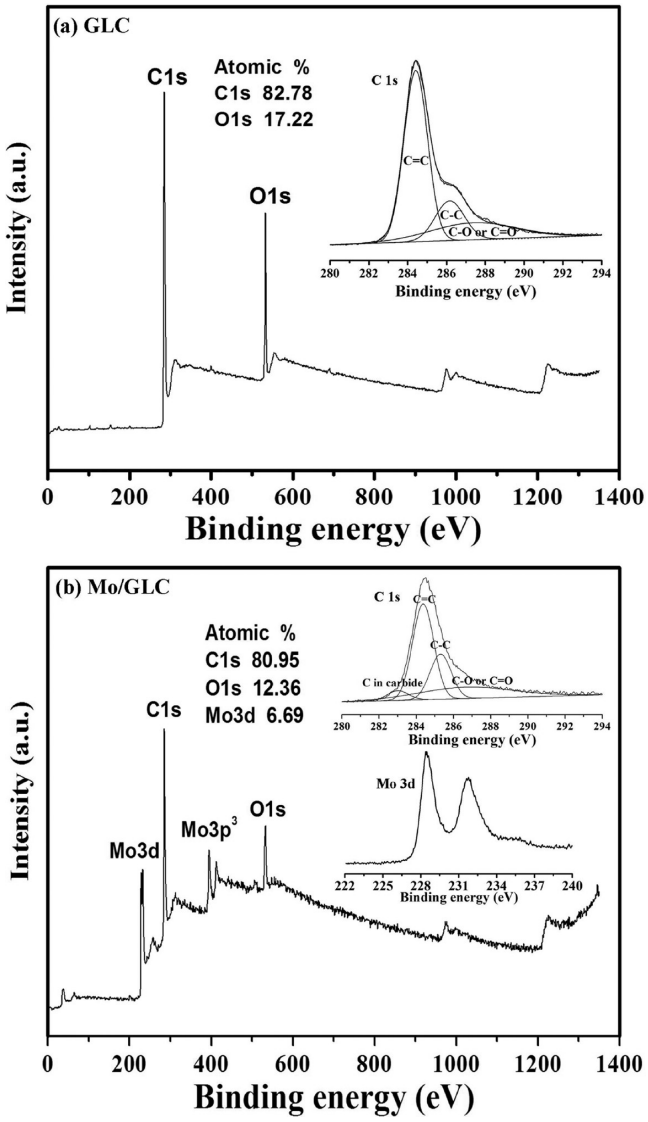

Figure 3. XPS survey scans for (a) GLC and (b) Mo-GLC films. Insets show C 1s and Mo 3d peak deconvolution.

2.2. Characterization. Field-emission scanning electron microscopy (FESEM; JEM-6701F) was used to observe surface morphology and cross-sectional features of GLC and Mo-GLC films. The wear tracks of samples are determined by scanning electron microscopy (SEM; JSM-5600LV) and the attached energy-dispersive spectroscopy microprobe (EDS), including the worn-out surface and the chemical composition of debris and its distribution. The chemical composition and microstructure of samples were evaluated by X-ray photoelectron spectroscopy (XPS; Physical Electronics) and Raman spectroscopy (HR800) in the cooperative way. Furthermore, the structure evolution of proteins was determined by Fourier transform infrared spectroscopy (FTIR; IFS 66 V/S) because of its high sensitivity to the secondary structure of proteins. The internal properties, mainly protein distribution and pore occurrence of the microparticles, were examined by transmission electron microscopy (TEM; TF20). Wear track profiles were analyzed using a noncontact 3D surface profiler (model MicroMAXTM, ADE Phase Shift, Tucson, AZ) after the wear test. A SVM3000 rotating viscometer was used to measure the density and viscosities of the physiological saline (PS), simulated body fluid (SBF), and fetal bovine serum (FBS) solutions at 37 °C. Each sample was measured at least three times and the average value was accepted. The nanohardness of as-deposited film on PEEK substrate was determined by the Nanotest600 nanoindenter apparatus (Micro Materials Ltd.), the indentation depth was set not to exceed 10% of the film thickness to ensure no interference from the substrate.

2.3. Friction and Wear Tests. A ball-on-disk reciprocating tribometer was applied to investigate the tribological properties of GLC and Mo-GLC films. All the friction measurements are done under the following conditions: an applied load of 3 N, a sliding speed of 10 cm/s, the counterpart Al_2O_3 ball with a diameter of 6 mm, the ambient humidity of 35%, and the room temperature of 23 °C. The dry friction media was ambient air, and the wet friction was performed in three biological lubricants, PS, SBF, and FBS, as shown in Figure 4. According to ref 29, the inorganic ion concentration of the SBF solution was nearly equal to that of human blood plasma (pH of 7.2−7.4 at 36.5−37 °C). The SBF solution contains biological macromolecules (trisaminomethane), while PS solution does not contain any organic biomacromolecules and was tested as a comparison with FBS solution. During the testing process, the ball-on-disk tribosystem was submerged into the fluids. Triplicate measures were done for each sample. The wear loss of the coating was calculated using the following formula on the basis of the 3D profile measurements:

$$K = \frac{V}{FL}(\mathrm{mm}^{-3}/\mathrm{N{\cdot}m}) \quad (1)$$

where V is the wear volume of GLC-coated substrates, F is the applied load, and L is the total sliding distance.

3. RESULTS

3.1. Friction and Wear Behaviors of Pure GLC and Mo-GLC Films in Different Biological Mediums. Figure 5

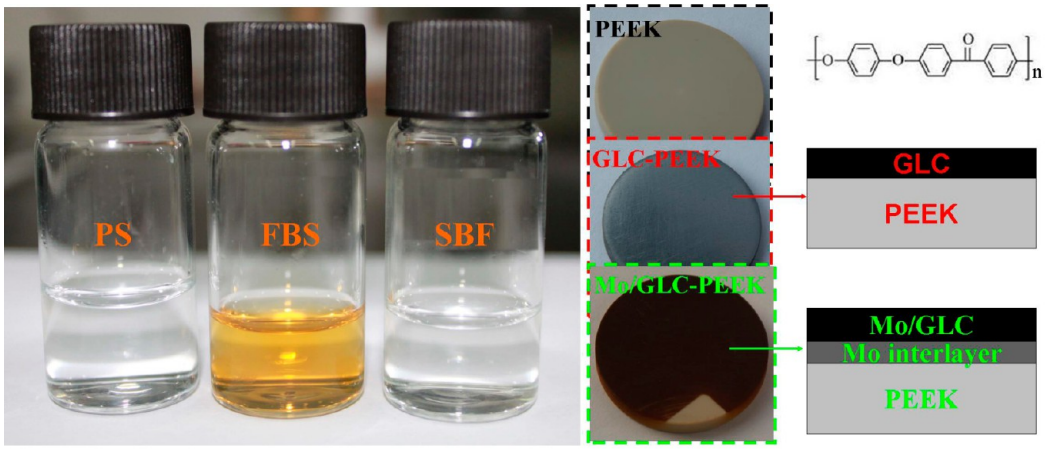

Figure 4. Photographs of three different biological fluids and the prepared samples.

DOI: 10.1021/am507850r
ACS Appl. Mater. Interfaces 2015, 7, 2772−2783

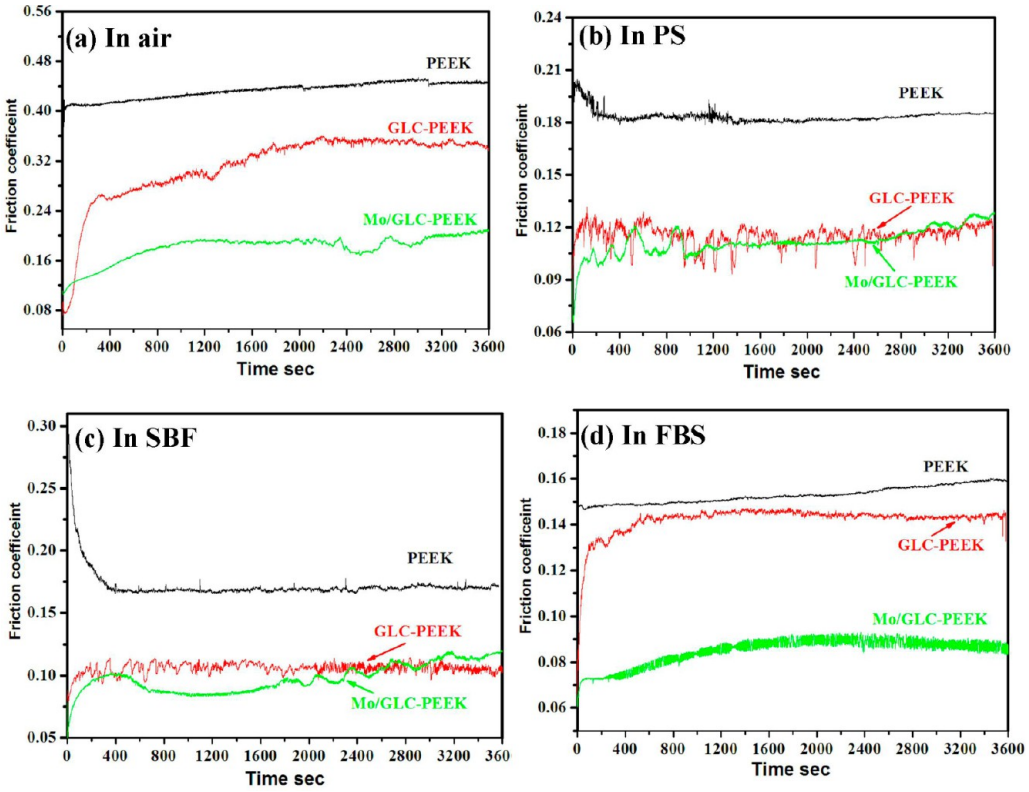

Figure 5. Frictional curves of PEEK, GLC−PEEK, Mo-GLC−PEEK in different biological environments: (a) in air, (b) in PS, (c) in SBF, and (d) in FBS.

shows a graph of the coefficient of friction as a function of time for pure GLC and Mo-GLC films against the Al_2O_3 counterpart in three biological fluids, and the dry friction of samples is tested as a comparison. Without lubricating fluids, PEEK shows a strongly fluctuating coefficient curve with an average friction coefficient of 0.45. On the contrary, the coated PEEK has a lower coefficient of friction (COF). However, the COF of pure GLC film starts out at approximately 0.08, followed by a sharp increase to 0.27. After a running-in period, the highest steady-state COF is about 0.35, which is believed to indicate the wear failure of the GLC film. When lubricated in the biological fluids, the friction coefficient of the sample remains approximately constant and tends to smaller values for the biological lubricant with higher viscosity. For PS and SBF solution, the variations of friction curves are almost identical for either pure GLC or Mo-GLC films. The frictional sliding curves of the film exhibit a large fluctuation during the whole experimental process. The fluctuation of friction curves might be ascribed to the combined effect of the chemicals in PS and SBF solution, friction force, and possible temperature rise. The friction coefficient of Mo-GLC film is much lower than that of pure GLC film. In FBS medium, the viscous protein sticks to the sliding surface of the films, and thus, the initial friction coefficients are relatively low, but upon increasing the sliding speed, the lubricating proteinaceous film gradually becomes thin and steady, so that the friction coefficient rises at first and then becomes stable. As can be seen from the figure, the friction curves of Mo-GLC film were much smoother, and the friction coefficient was more stable and lower as compared with that of the other three media. The friction coefficient of PEEK reaches the highest value at about 0.16 compared to 0.14 and 0.09 measured for pure GLC and Mo-GLC film, respectively, but it is worth noting that the friction coefficient of pure GLC film under FBS solution was higher than that for Mo-GLC film. In addition, the graphitization effect or tribolayers of amorphous carbon films played a vital role in the solid−liquid composite lubricating effect, which contributed to the further reduction of friction.

Figure 6 gives the corresponding average COF of the uncoated and coated PEEK in different environments. We could observe clearly that the average COF of the uncoated and coated PEEK under dry sliding is the highest and under fetal bovine serum is the lowest. Under the three biological fluid conditions the average COF of all samples follows the rule of $\mu_{\text{in FBS}} < \mu_{\text{in SBF}} < \mu_{\text{in PS}}$, which can be related to the higher

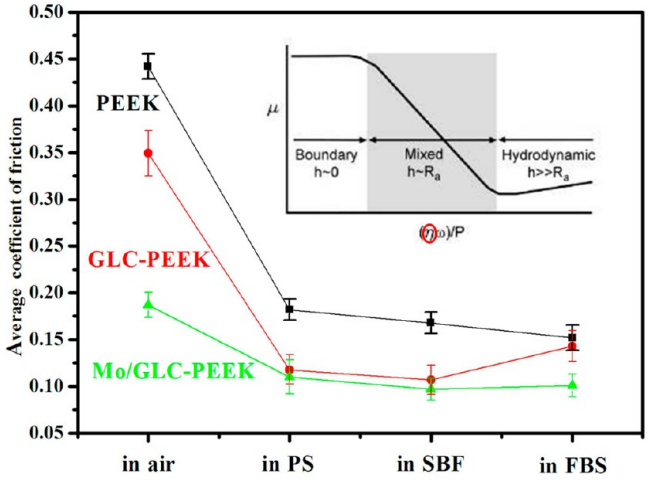

Figure 6. Average friction coefficient of PEEK, GLC−PEEK, and Mo-GLC−PEEK under different environmental conditions.

DOI: 10.1021/am507850r
ACS Appl. Mater. Interfaces 2015, 7, 2772−2783

viscosity of FBS solution resulting in the apparent decrease of the friction coefficient. According to the Stribeck curve, the friction coefficient is inversely proportional to a normal load (P) and directionally proportional to the velocity (ω) and viscosity (η) of the lubricant.[30] The viscosity of the three media increased in the following order: PS < SBF < FBS. Under the present testing conditions, if a mixed lubrication or/and boundary lubrication regime might be considered, we believe that this effect can be attributed to the presence of an adsorbed proteinaceous film at the liquid/solid interfaces.

In this paper, an equivalent ball-on-plane model was used to represent the articulation, simply defined by the effective radius (R') and elastic modulus (E').

$$R' = R_1 = 6\ \text{mm} \tag{2}$$

$$\frac{1}{E'} = \frac{1}{2}\left(\frac{1-\nu_{\text{films}}{}^2}{E_{\text{films}}} + \frac{1-\nu_{\text{ball}}{}^2}{E_{\text{ball}}}\right) \tag{3}$$

The corresponding lubrication regime can be approximately predicted according to the λ ratio in eq 4, where $h_{\min}$ corresponds to the minimum film thickness. The Hamrock–Dowson equation for isoviscous and elastic lubrication in eq 5 is well-known,[31] and Rq′ is the composite roughness evaluated by eq 6

$$\lambda = \frac{h_{\min}}{\text{Rq}'} \tag{4}$$

$$h_{\min} = 2.8R'\left(\frac{\eta u_e}{E'R'}\right)^{0.65}\left(\frac{W_y}{E'R'^2}\right)^{-0.21} \tag{5}$$

$$\text{Rq}' = \sqrt{R_{\text{ball}}{}^2 + R_{\text{film}}{}^2} \tag{6}$$

where W_y is the normal load, R' is the radius of the ball (6 mm), E_{ball} and ν_{ball} are the elastic modulus and Poisson's ratio of the Al_2O_3 ball, and E_{films} and ν_{film} are the elastic modulus and Poisson's ratio of the Mo-GLC film. The specific parameters are reported in Table 1. Once the λ ratio is evaluated, the lubrication regime is conventionally identified by the following ranges: $0.1 < \lambda < 1$ shows boundary lubrication; $1 \le \lambda \le 3$ shows mixed lubrication, and $\lambda > 3$ shows full film lubrication.

Table 1. Mechanical Properties of Materials and Typical Roughness Values for Ball-on-Plane Equivalent Configuration: The Elastic Modulus (E), Poisson's Ratio (ν), and Average Roughness (R_a)

material	E (GPa)	ν	R_a (μm)	E' (GPa)
ball: Al_2O_3	210	0.3	0.02	
plane: PEEK	3.6	0.25	3	7.55
GLC	25.2	0.25	0.58	48.17
Mo-GLC	32.6	0.25	0.3	60.42

Considering an average vertical load W_y = 3 N, a flexion extension velocity u_e = 10 cm/s, and the viscosity values of PS, SBF, and FBS of 0.65, 0.86, and 0.95 mPa s at 37 °C, λ obtained from eq 4 for the bearings in Table 1 are reported in Table 2 and their lubrication regime was estimated. Typically, tribochemical reactions are essential for tribosystems running under boundary or mixed lubrication conditions.

The wear volumes were calculated from the wear track profile obtained using a noncontact 3D surface profiler three times. The wear rates of the Mo-doped GLC-coated PEEK under different experimental conditions are shown in Figures 7–10. Under dry sliding condition, the uncoated PEEK presents a relatively high wear rate, which is 6.43×10^{-6} mm^3/N·m. However, the as-fabricated Mo-GLC film has a very low wear rate of 1.87×10^{-6} mm^3/N·m, which is just one-third of that for the uncoated PEEK. Additionally, the insets in Figure 7 are their corresponding wear tracks, and it can be seen that the uncoated PEEK has a comparatively deep wear track, typical characteristics of adherence and scratches on the wear surface. For GLC-coated PEEK, the SEM images reveal a severely damaged wear track and some delamination. Especially, it presents the widest and deepest wear track. For Mo-GLC–PEEK, the wear track is very narrow and shallow. From the right of Figure 7, it can be seen that the corresponding Al_2O_3 ball mated with Mo-GLC film shows the smallest wear scar, although lots of wear debris is aggregated beside the wear scars of the ball along the wear orientation. In PS solution (Figure 8), the specific wear rate of the uncoated PEEK is approximately 2.03×10^{-6} mm^3/N·m, which is reduced greatly to around 1.19×10^{-6} and 0.97×10^{-6} mm^3/N·m by GLC and Mo-GLC films, respectively. The surface of the polymer PEEK is heavily damaged by plowing, which leads to deep and wide furrows as well as serious plastic deformation near the surface. However, slight wear and a rather smooth surface with smaller damaged regions are presented for GLC and Mo-GLC films. Besides, because the hardness of GLC (3.83 GPa) and Mo-GLC (5.62 GPa) films are higher than uncoated PEEK (0.24 GPa), quite larger wear scars on the corresponding Al_2O_3 balls are clearly observed when compared with that for uncoated PEEK. In addition, the contact region is damaged with the formation of a wear scar and the deposited NaCl crystal on the surface of the Al_2O_3 balls. In SBF solution (Figure 9), the wear rates of uncoated PEEK are always significantly higher than those of coated PEEK. It has been calculated that the specific wear rate of uncoated PEEK is approximately 1.6×10^{-6} mm^3/N·m, whereas the specific wear rate of GLC and Mo-GLC–PEEK are approximately 1.18×10^{-6} and 0.76×10^{-6} mm^3/N·m, respectively. The plastic deformation and furrows are more obvious on the worn surface of uncoated PEEK. The wear tracks on the GLC and Mo-GLC films after sliding tests had a similar morphology, and no spallation or delamination could be detected. Seen from the typical 3D morphologies, the difference of wear depth between uncoated and coated PEEK can be seen clearly. In FBS solution (Figure 10), the wear rate values are about 1.43×10^{-6}, 0.69×10^{-6}, and 0.62×10^{-6} mm^3/N·m, corresponding to PEEK, GLC–PEEK, and Mo-GLC–PEEK, respectively. The wear rate

Table 2. Ranges of λ, Minimum Film Thickness ($h_{\min}$), and Lubrication Regime Are Calculated on the Basis of Rq′ range

material	medium	$h_{\min}$ (μm)	λ	lubrication regime
PEEK	PS	0.3	0.125	boundary lubrication
	SBF	0.36	0.15	
	FBS	0.39	0.16	
GLC–PEEK	PS	0.133	0.22	boundary lubrication
	SBF	0.159	0.266	
	FBS	0.17	0.283	
Mo-GLC–PEEK	PS	0.12	0.42	boundary lubrication
	SBF	0.14	0.51	
	FBS	0.15	0.54	

DOI: 10.1021/am507850r
ACS Appl. Mater. Interfaces 2015, 7, 2772–2783

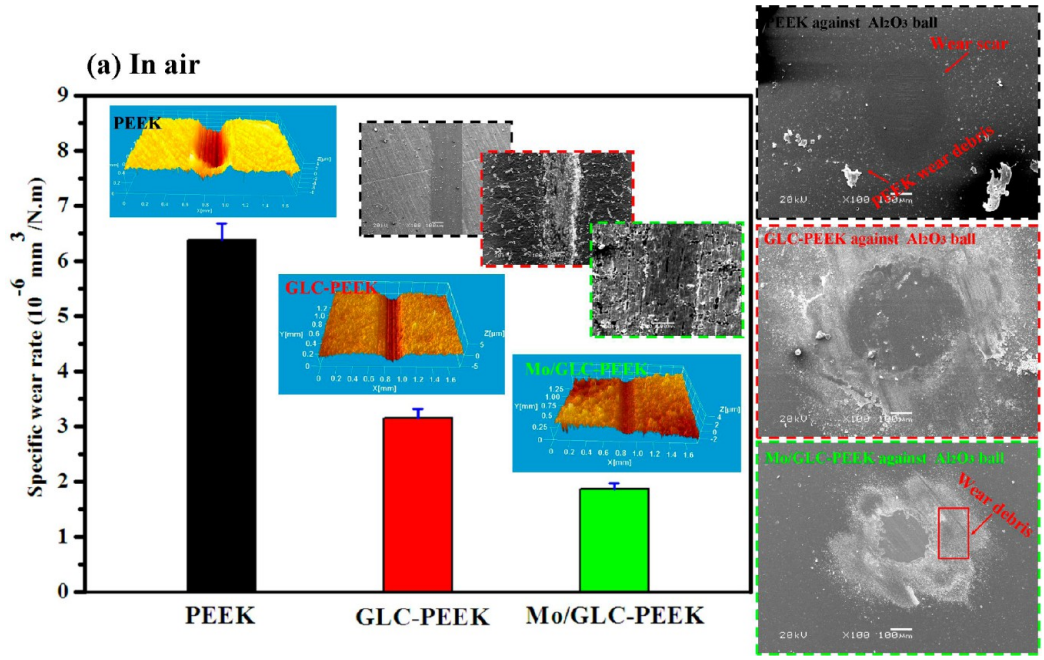

Figure 7. Wear rates of PEEK, GLC−PEEK, and Mo-GLC−PEEK and wear scars of mating Al_2O_3 balls in air.

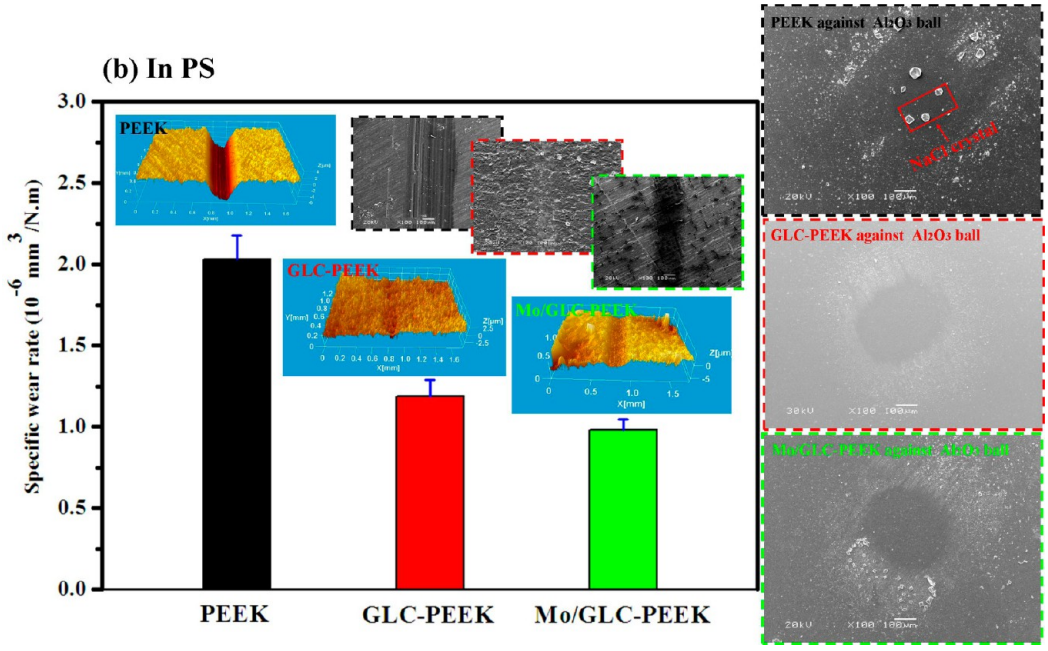

Figure 8. Wear rates of PEEK, GLC−PEEK, and Mo-GLC−PEEK and wear scars of mating Al_2O_3 balls in PS.

of all the samples are lower than in PS and SBF solution, due to the protective and lubricating role of the protein. The corresponding wear track of Mo-GLC film shows the wear depth as shallow as the level of film surface roughness. However, a severely damaged surface is measured for pure GLC, with spalling or delamination. Almost no wear took place on the surface of the Al_2O_3 ball in FBS solution due to the boundary lubrication of the protein, as shown in Figure 10. Meanwhile, the surface of the Al_2O_3 ball was covered with a continuous solid proteinaceous layer after 1 h of sliding, which may be caused by the adsorbed proteins. As the experimental results indicated, the wear rates of uncoated PEEK are higher than those of the coated ones under all experimental conditions considered, and all the samples yield the lowest wear rates under FBS solution and the highest under dry sliding conditions.

In order to validate the elemental compositions of the surface adsorbed on the Al_2O_3 ball, the adsorbed layer was evaluated by utilizing EDS analysis. Figure 11 illustrates the schematic diagram of the friction reduction mechanism of Mo-GLC films and EDS analysis under different experimental conditions. As presented by Figure 11a, most of those dangling strong covalent σ-bonds are terminated during dry sliding contact by C═O, C−H, and C−OOH bonds. This is mainly due to the adsorption and dissociation of oxygen and water molecules on the surface of the Mo-GLC film.[32] The relatively small friction

DOI: 10.1021/am507850r
ACS Appl. Mater. Interfaces 2015, 7, 2772−2783

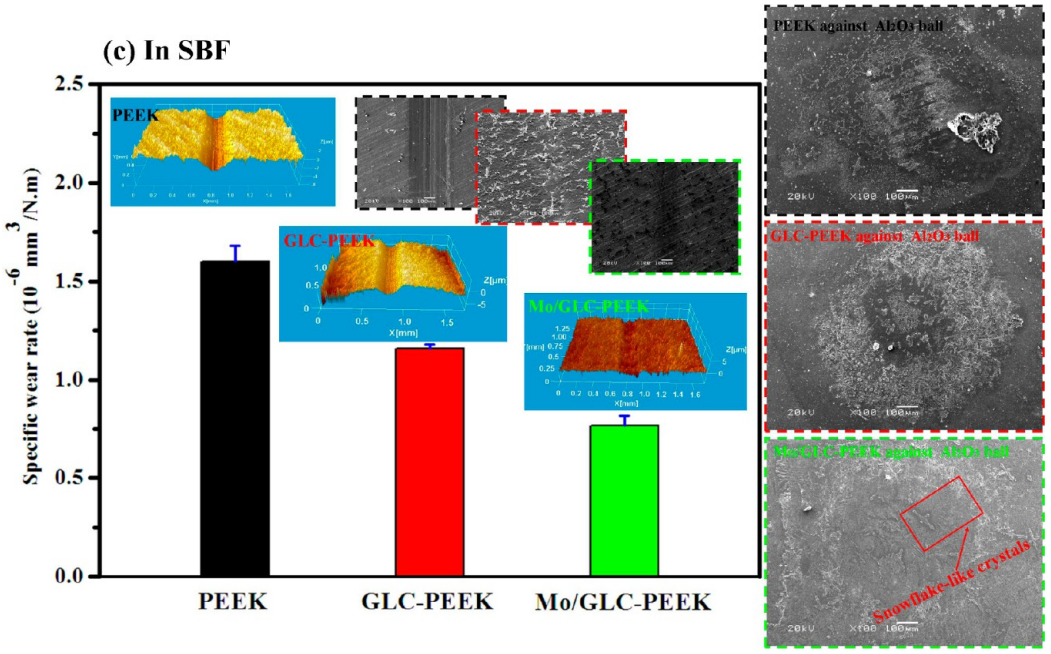

Figure 9. Wear rates of PEEK, GLC−PEEK, and Mo-GLC−PEEK and wear scars of mating Al_2O_3 balls in SBF.

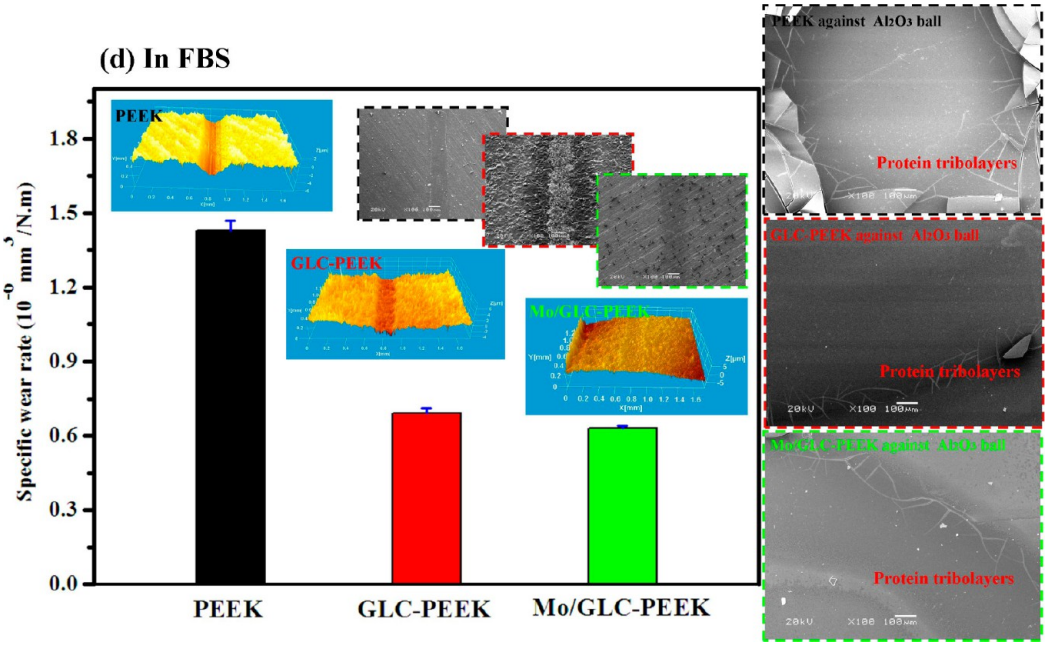

Figure 10. Wear rates of PEEK, GLC−PEEK, and Mo-GLC−PEEK and wear scars of mating Al_2O_3 balls in FBS.

of the water molecules in some contact areas results in the formation of strong carbon−carbon covalent bonds, which can increase the adhesive interaction and thus make the friction coefficient relatively higher in ambient air. However, PS and SBF solutions provide a large number of water molecules, so almost all of the dangling σ-bonds are terminated by C═O, C−H, and C−OOH bonds. Because of the existence of effective lubrication, the Mo-GLC film and Al_2O_3 ball cannot easily directly contact each other. Therefore, the friction force would be the van der Waals force and the hydrogen-bonding interaction between water molecules and tribopair, which leads to a very low friction coefficient. Meanwhile, some new elements were detected by EDS, such as Na, Mg, K, Ca, and Cl; the carbon, hydrogen, and oxygen were derived from the lubricants. In SBF solution, a continuous snowflake-like crystals film was present on the contact area, which could protect the contacting surfaces from rubbing each other. In FBS solution, the surface of the Al_2O_3 ball was covered with a continuous solid layer, which may be caused by a tribolayer of proteins. The tribolayer of proteins can act as low-shear-modulus boundary lubrication additives during sliding friction. Additionally, N and S elements were obtained from the continuous solid layers surface. Therefore, the ceramic surface underneath appeared relatively smooth.

3.2. Analysis of FBS Solution after Sliding Tests. After the wear tests, FBS solution is collected and stored. As seen

DOI: 10.1021/am507850r
ACS Appl. Mater. Interfaces 2015, 7, 2772−2783

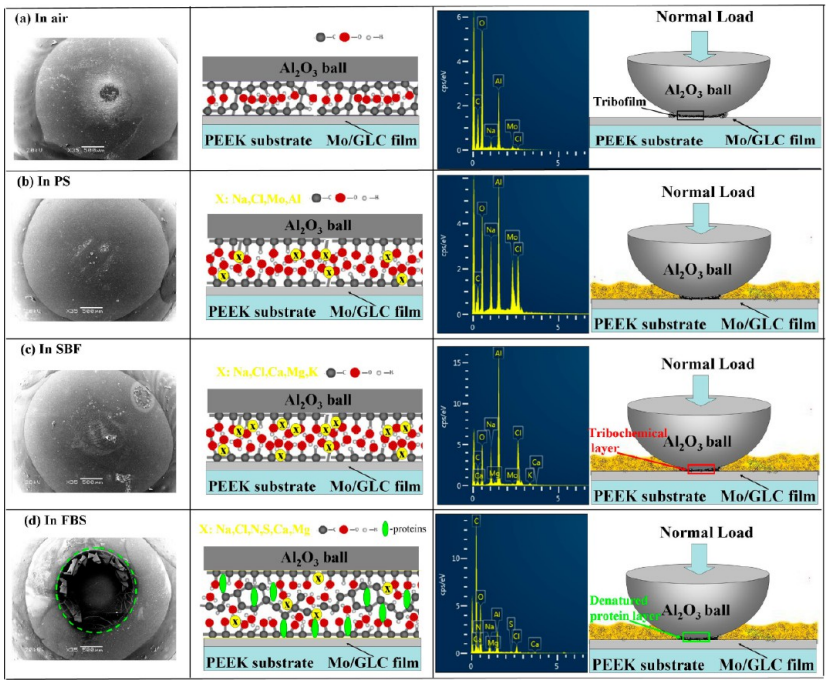

Figure 11. Schematic drawing of the friction mechanism of the film in different environments: (a) in ambient air, (b) in PS, (c) in SBF, (d) in FBS.

with the naked eye, light to dark colors are present in the FBS solution after the sliding wear test, and a large number of black precipitate particles are dispersed and then precipitated, which possibly are a mixture of small graphite-like wear particles and protein that is thermally denatured as a result of material contact.[33] Figure 12b shows FTIR spectra of bovine serum before and after the friction test. FTIR spectroscopy was the most often used method for obtaining relevant information on the protein misfolding and aggregation in vitro.[34−36] It should be noted that two prominent features appear in a protein, one is the amide I band and the other one is the amide II band. The amide I region (1600−1700 cm^{-1}) band is the stretching vibrations of C═O (approximately 80%) coupled weakly with C−N stretch and N−H bending,[37] which are mainly affected during conformational changes in the protein secondary structure. So the frequency of the amide I vibrational mode is particularly sensitive to secondary structure. For example, in the α-helical structure, the main amide I absorbance is around 1655 cm^{-1}, while for the β-sheet peak it is normally around 1630 cm^{-1}, and random coil structures occur at around 1644 cm^{-1}.[35,38] Especially, the vibrational frequency of an aggregated protein falls around 1620−1625 cm^{-1} due to the distinct hydrophobic environment.[39] The amide II region (1500−1600 cm^{-1}) band is mainly derived from the C−N (approximately 40%) stretch along with N−H (approximately 60%) in-plane bending.[40] Strong confirmation can be obtained from TEM analysis in Figure 12c that the protein aggregation and misfolding are seen for some of the FBS solutions with the dimensions ranging from tens to hundreds of nanometers. Additionally, protein aggregates are usually very small and the initial oligomers form at the nanoscale. The aggregates gradually become larger or greater, but the largest of them are only 20−30 μm in size. Meanwhile, the spectral differences can capture a subtle protein conformational change requiring spectra with a high signal-to-noise ratio (S/N).[41] Reference 33 has shown that these tribolayers are rich in organic carbon, originating from the joint fluid, in addition to metal oxides and a number of organic elements and salts.

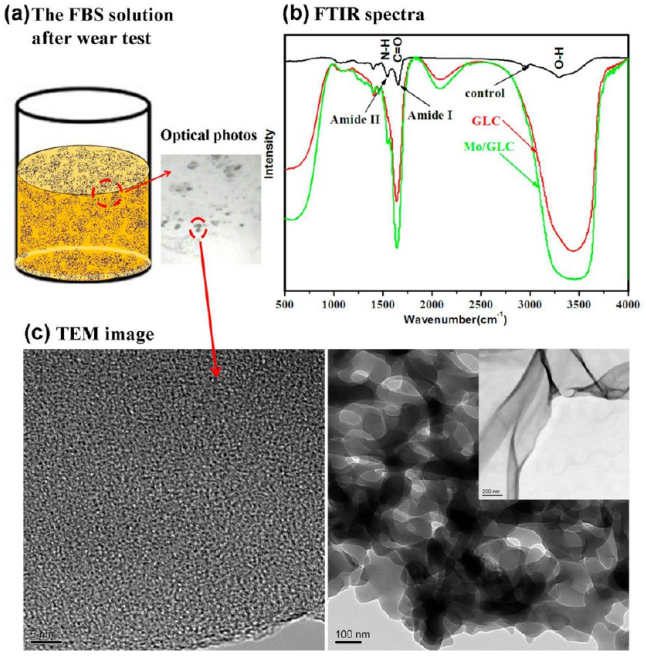

Figure 12. (a) The FBS solutions after the wear test, (b) FTIR spectra of FBS solution after the wear rest, and (c) TEM image of the protein aggregates.

3.3. Analysis of the Contact Surface of Mo-GLC Film under FBS Solution. To further analyze the surface coverage of Mo-GLC film after the sliding wear test under FBS solution, the wear track zone can be resolved by means of XPS spectra, as shown in Figure 13. The presence of elemental N or N-containing fragment ions indicates proteins adsorbed to surfaces. The binding energies of N 1s detected on the surface of Mo-GLC film (close to 400 eV) are typical for organic

DOI: 10.1021/am507850r
ACS Appl. Mater. Interfaces 2015, 7, 2772−2783

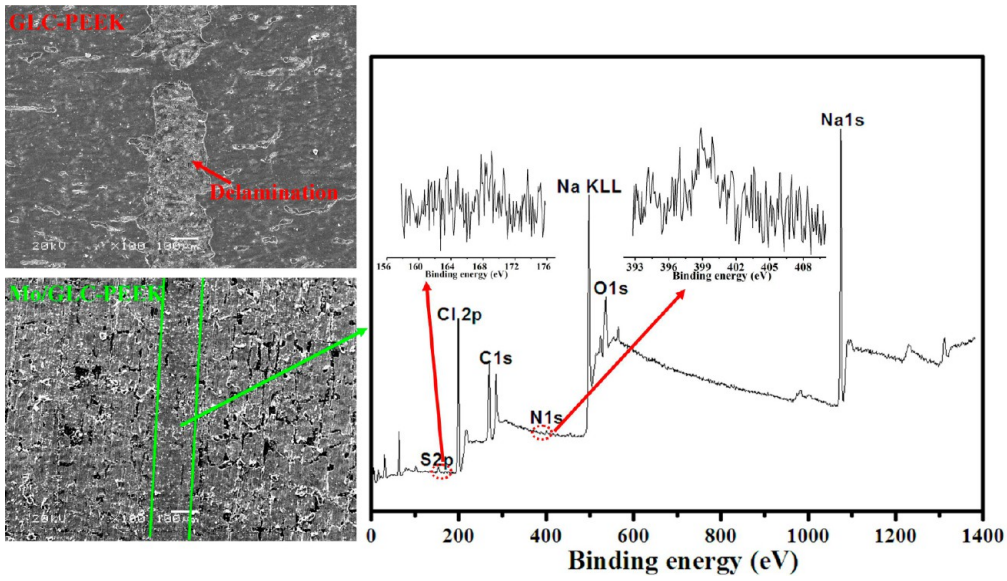

Figure 13. XPS spectra of the surface of Mo-GLC film after the wear test under FBS.

matrices and are related to C−N bonds.[42,43] Furthermore, the detection of sulfur (S 2p centered at 169 eV) is assigned to cysteine and methionine amino acids. The presence of Na 1s and Cl 2p peaks in the sample may be from the FBS solution. So the wear performance of Mo-GLC film might be affected by the organic components. The proteins in FBS solution can form a proteinaceous tribolayer on the surface of Mo-GLC film, currently often called the biofilms or tribological films.[44] The tribofilm is carbonaceous. It can act as a solid lubricant and can also act as a barrier to prevent further wear.

4. DISCUSSION

Generally, the antiwear ability and low friction coefficient of GLC films are strongly dependent on the interfacial graphitization at microcontact regions under dry conditions,[45] and such results can be found in this study. It has been known that tribochemical reactions of the artificial joint interface with the surroundings media are inevitable and that physiological fluids could be pumped into the prosthesis implants interface under physiological loading. Therefore, a further understanding of the tribochemcal reactions of biological lubrication is necessary. Under PS lubrication, the friction coefficients for uncoated and coated PEEK are lower than under dry sliding conditions. This can be explained by the aqueous medium affecting the tribological behavior of uncoated PEEK during the sliding wear testing. For the uncoated PEEK, when it is subjected to cross-directional shearing, the ripples on PEEK are more easily broken off. Therefore, more wear debris will be flushed away and a higher wear mass loss of plain PEEK will be induced (Figure 8). Besides, PS solution contains a large number of chloride ions that can greatly accelerate the corrosion of the mating ball surface, and the corrosion of the counterface would further deteriorate the lubricating effect of PS solution and then significantly increase the plow breakage to plain PEEK. So the wear mass loss of plain PEEK increases too much. Though the PEEK wear debris got continuously flushed by the PS solution, the actual wear rates and the wear volumes in PS solution were lower than in dry friction media. As analyzed above, we can conclude that the main wear mechanism of plain PEEK is abrasive wear characterized by the plowing effect in PS solution, while adhesive wear is the main wear mechanism under dry sliding conditions. However, for the coated PEEK, on the one hand, the solution provides a large amount of water molecules, so almost all of the dangling σ-bonds are terminated by C═O, C−H, and C−OOH bonds.[46] In other words, the low friction is due to the formation of hydroxyl and carboxyl groups on the film surfaces preventing the adhesion between the sliding materials. Because of the formed hydrophilic groups, the film and the mating ball cannot easily directly contact each other. In addition to medium lubrication, the carbon-based film is a solid self-lubricating material, which has good lubrication itself.

When sliding in the SBF solution, there is a large amount of accumulated materials around the wear scar of the Al_2O_3 ball compared to the test condition with PS solution. The accumulated materials were the corrosion products of the film material from the SBF solution, which protected the surface of counterface ball, and therefore, the ball had less wear loss, as shown in Figure 9. For the better tribological performance of the SBF solution, besides the reasons of the terminated dangling σ-bonds and the low chloride ion concentration, another major reason is that the SBF solution contains larger amount of Ca^{2+} and Mg^{2+}. As presented by Figure 11c, EDS analysis indicated that the main components of SBF solution are Ca^{2+} and Mg^{2+}, which result in the relatively low wear rate and friction coefficient of all films in SBF solution, because the deposited layer of $CaCO_3$ (or CaO) and $Mg(OH)_2$ acted as the lubrication layer.[47,48] Meanwhile, the lubrication layer can isolate the Al_2O_3 ball surface with SBF solution as well as prevent oxygen (O_2) and chloride ion (Cl^-) from diffusing onto the surface of the Al_2O_3 ball, thus reducing the corrosion of the mating ball. Moreover, it has been reported[49] that the inorganic ions such as HPO_4^{2-} and H_2PO^{4-} present in the composition of the SBF solution could be adsorbed on the film surface, decreasing the interaction between the film and the corrosive solution, but the mating Al_2O_3 balls are covered with a thinner layer of corrosion products.

The way in which the protein-containing biological environments affect the performance of prosthetic materials is of interest to many researchers. Compared to PS and SBF

DOI: 10.1021/am507850r
ACS Appl. Mater. Interfaces 2015, 7, 2772−2783

solution, FBS solution supplies a protein-rich environment. As soon as the film is immersed in FBS solution, the adsorbed protein layer at wear zone can reduce the direct contact between the Al_2O_3 ball and the film and function as a semiprotective film, improving the boundary lubrication. Particularly, the adsorbed protein at the real contacting protuberant point will suffer from an elevated temperature, namely, when the temperature-induced denaturation of proteins occurs. The denaturing of the protein is always irreversible, which means it cannot go back to its original state.[50] Therefore, the formation of these protein aggregates or precipitates could be due to the frictional heat and/or high-shear-induced protein denaturation within the tribocontact, and the denatured protein shown in Figure 12c mixed with the graphite-like debris may further protect the film and counterface surface. Once the tribological process starts,[6] the nature of the proteins can be changed, turning them into a lubricating film. As shown in Figure 10, it can be seen that the wear scar of the Al_2O_3 ball was covered with a thick protein solidlike film after 1 h of sliding. It protects the Al_2O_3 ball from contacting the films directly and results in a reasonable reduction of the surface wear and surface damage. Furthermore, the surface of the Mo-GLC film was coated with a proteinaceous film, as evidenced by the significant peak of nitrogen and sulfur contents (Figure 13), which are considered indicators of protein adsorption. This evidence indicates that the solid film was indeed adsorbed proteins from the fetal bovine serum solution, as the amide bond (−CONH−) is the basic unit of protein, which has been addressed by many authors.[51,52] In our own studies, this is believed to be the result of the formation of solidlike films resulting from the tribochemical reaction of proteins with the corresponding ball. However, studies showed such a lubricating effect of proteinaceous film would be beneficial in terms of wear but can either increase or decrease the friction between the contacting surfaces.[51,53] This is supported by other researchers who have shown that low wear rates of films against ball are contributed by the deposition of protein and other organic contents in human serum.[46,54] Interestingly, the different molecular structures of different proteins have different adsorption properties with the different implant materials and a different effect on the tribological behavior.

An important factor that influences the protective character of GLC films is their adhesion to the substrate, since it has significant influences on the bearing capacity and the wear life of the films. SEM micrographs and friction curves together revealed that the tribological properties for the Mo-GLC film were better than those of pure GLC film and uncoated PEEK, irrespective of working media and load conditions. From Figure 13, if the film was not prepared properly, pieces of GLC film peel off the PEEK substrate under cyclic stress in combination with the corrosion of FBS solution. This is mainly due to pure GLC films poorly adhesing to PEEK substrate and the viscosity of FBS solution, which should be directly responsible for the shortest wear life. Fortunately, the typical amorphous microstructure of GLC allows the doping with nonmetal and metal elements, such as Si,[55] Ti,[56] or Ag,[57] to improve the proper functionality for biomaterial application. In this work, the Mo interlayer bonds well with both the GLC film and PEEK substrate. Furthermore, the antiwear and antifriction characteristics of Mo-GLC film could be more advantageous for the surface protection of PEEK. The role of medium on the synergistic interaction between film and counterface needs particular attention.

5. CONCLUSIONS

In conclusion, this work revealed that Mo-doped GLC film improved antifriction and antiwear properties and the stability in biological environments. The findings indicated that the friction coefficient of Mo-GLC film under all experimental conditions was lower than that on pure GLC film. Under dry sliding condition, because of the absence of biological lubricants and the formation of covalent bonds between tribopair, all the films have both high wear rate and friction coefficient. In PS and SBF solution, the films have lower friction coefficient and a lower wear rate than that in air because of the presence of the tribochemical reactions products and the lubrication of biological media. In FBS solution, the films have the lowest friction coefficient and wear rate, which is brought about by means of the boundary lubrication effect of the thick protein solidlike films.

AUTHOR INFORMATION

Corresponding Author

*Tel: +86-0931-4968080. E-mail: lpwang@licp.cas.cn.

Notes

The authors declare no competing financial interest.

ACKNOWLEDGMENTS

The authors are grateful for financial support from the National Natural Science Foundation of China (No. 51322508&11172300).

REFERENCES

(1) Herberts, P.; Malchau, H. Long Term Registration Has Improved the Quality of Hip Replacement: A Review of the Swedish THR Register Comparing 160,000 Cases. *Acta Orthop. Scand.* **2000**, *71*, 111−121.

(2) Eschbach, L. Nonresorbable Polymers in Bone Surgery. *Injury* **2000**, *31*, 22−27.

(3) Katzer, A.; Marquardt, H.; Westendorf, J.; Wening, J. V.; von Foerster, G. Polyetheretherketone−Cytotoxicity and Mutagenicity in Vitro. *Biomaterials* **2002**, *23*, 1749−1759.

(4) Purdue, P. E.; Koulouvaris, P.; Nestor, B. J.; Sculco, T. P. The Central Role of Wear Debris in Periprosthetic Osteolysis. *HSS J.* **2006**, *2*, 102−113.

(5) Goodman, S. B. Wear Particles, Periprosthetic Osteolysis and the Immune System. *Biomaterials* **2007**, *28*, 5044−5048.

(6) Liao, Y.; Pourzal, R.; Wimmer, M. A.; Jacobs, J. J.; Fischer, A.; Marks, L. D. Graphitic Tribological Layers in Metal-on-Metal Hip Replacements. *Science* **2011**, *334*, 1687−1690.

(7) O'Brien, B.; Stinson, J.; Carroll, W. Development of a New Niobium-Based Alloy for Vascular Stent Applications. *J. Mech. Behav. Biomed. Mater.* **2008**, *4*, 303−312.

(8) Matsuno, H.; Yokoyama, A.; Watari, F.; Uo, M.; Kawasaki, T. Biocompatibility and Osteogenesis of Refractory Metal Implants, Titanium, Hafnium, Niobium, Tantalum and Rhenium. *Biomaterials* **2001**, *22*, 1253−1262.

(9) Geringer, J.; Forest, B.; Combrade, P. Fretting-Corrosion of Materials Used as Orthopaedic Implants. *Wear* **2005**, *259*, 943−951.

(10) Prete, P. E.; Gurakar-Osborne, A.; Kashyap, M. L. Synovial Fluid Lipids and Apolipoproteins: A Contemporary Perspective. *Biorheology* **1995**, *32*, 1−16.

(11) Mattei, L.; DiPuccio, F.; Piccigallo, B.; Ciulli, E. Lubrication and Wear Modelling of Artificial Hip Joints: A Review. *Tribol. Int.* **2011**, *44*, 532−549.

DOI: 10.1021/am507850r
ACS Appl. Mater. Interfaces 2015, 7, 2772−2783

(12) Hu, C. C.; Liau, J. J.; Lung, C. Y.; Huang, C. H.; Cheng, C. K. A Two Dimensional Finite Element Model for Frictional Heating Analysis of Total Hip Prosthesis. *Mater. Sci. Eng., C* **2001**, *17*, 11−18.
(13) Huang, J. X.; Wan, S. H.; Liu, B.; Xue, Q. J. Improved Adaptability of PEEK by Nb Doped Graphite-like Carbon Composite Coatings for Bio-Tribological Applications. *Surf. Coat. Technol.* **2014**, *247*, 20−29.
(14) Tiainen, V. M. Amorphous Carbon as a Bio-Mechanical Coating-Mechanical Properties and Biological Applications. *Diamond Relat. Mater.* **2001**, *10*, 153−160.
(15) Sheeja, D.; Tay, B. K.; Lau, S. P.; Nung, L. N. Tribological Characterisation of Diamond-like Carbon Coatings on Co−Cr−Mo Alloy for Orthopaedic Applications. *Surf. Coat. Technol.* **2001**, *146−147*, 410−416.
(16) Scholes, S. C.; Unsworth, A.; Hall, R. M.; Scott, R. The Effects of Material Combination and Lubricant on the Friction of Total Hip Prostheses. *Wear* **2000**, *241*, 209−213.
(17) Heuberger, M. P.; Widmer, M. R.; Zobeley, E.; Glockshuber, R.; Spencer, N. D. Protein-Mediated Boundary Lubrication in Arthroplasty. *Biomaterials* **2005**, *26*, 1165−1173.
(18) Gispert, M. P.; Serro, A. P.; Colaco, R.; Saramago, B. Friction and Wear Mech-anisms in Hip Prosthesis: Comparison of Joint Materials Behavior in Several Lubricants. *Wear* **2006**, *260*, 149−158.
(19) Chandrasekaran, M.; Loh, N. L. Effect of Counterface on the Tribology of UHMWPE in the Presence of Proteins. *Wear* **2001**, *250*, 237−241.
(20) Mishina, H.; Kojima, M. Changes in Human Serum Albumin on Arthroplasty Frictional Surfaces. *Wear* **2008**, *265*, 655−663.
(21) Johnson, J. L.; Jones, H. P.; Rajagopalan, K. V. In Vitro Reconstitution of Demolybdosulfite Oxidase by a Molybdenum Cofactor from Rat Liver and Other Sources. *J. Biol. Chem.* **1977**, *252*, 4994−5003.
(22) Turnlund, J. R.; Friberg, L. T. *Handbook on the Toxicology of Metals*; Nordberg, G. F., Fowler, B. A., Nordberg, M., Eds.; Elsevier B.V.: New York, 2007; Chapter 34, pp 731−741.
(23) Afkhami, A.; Norooz-Asl, R. Removal, Preconcentration and Determination of Mo(VI) from Water and Wastewater Samples using Maghemite Nanoparticles. *Colloids Surf., A* **2009**, *346*, 52−57.
(24) Ferrari, A. C.; Robertson, J. Raman Spectroscopy of Amorphous, Nanostructured, Diamond-like Carbon, and Nanodiamond. *Philos. Trans. Math. Phys. Eng. Sci.* **2004**, *362*, 2477−2512.
(25) Gradowski, M. V.; Ferrari, A. C.; Ohr, R.; Jacoby, B.; Hilgers, H.; Schneider, H. H.; Adrian, H. Resonant Raman Characterisation of Ultra-Thin Nano-Protective Carbon Layers for Magnetic Storage Devices. *Surf. Coat. Technol.* **2003**, *174*, 246−252.
(26) Ji, L.; Li, H. X.; Zhao, F.; Chen, J. M.; Zhou, H. D. Microstructure and Mechanical Properties of Mo/DLC Nanocomposite Films. *Diamond Relat. Mater.* **2008**, *17*, 1949−1954.
(27) Moulder, J. F.; Stickle, W. F.; Sobol, P. E.; Bomben, K. D. *Handbook of X-ray Photoelectron Spectroscopy*; Perkin-Elmer Corp.: Eden Prairie, MN, 1992.
(28) Baba, K.; Hatada, R. Preparation and Properties of Metal-Containing Diamond-like Carbon Films by Magnetron Plasma Source Ion Implantation. *Surf. Coat. Technol.* **2005**, *196*, 207−210.
(29) Kokubo, T.; Takadama, H. How Useful is SBF in Predicting in Vivo Bone Bioactivity? *Biomaterials* **2006**, *27*, 2907−2915.
(30) Gleghorn, J. P.; Bonassar, L. J. Lubrication Mode Analysis of Articular Cartilage Using Stribeck Surfaces. *J. Biomech.* **2008**, *9*, 1910−1918.
(31) Jin, Z. M.; Dowson, D.; Fisher, J. Analysis of Fluid Film Lubrication in Artificial Hip Joint Replacements with Surfaces of High Elastic Modulus. *Proc. Inst. Mech. Eng. H.* **1997**, *211*, 247−256.
(32) Donnet, C.; Erdemir, A. *Tribology of Diamond-Like Carbon Films: Fundamentals and Applications*; Springer: New York, 2008; p 155. ISBN: 978-0-387-30264-5 (print), 978-0-387-49891-1 (online).
(33) Hesketh, J.; Ward, M.; Dowson, D.; Neville, A. The Composition of Tribofilms Produced on Metal-on-Metal Hip Bearings. *Biomaterials* **2014**, *35*, 2113−2119.
(34) Ong, J. L.; Chittur, K. K.; Lucas, L. C. Dissolution/Reprecipitation and Protein Adsorption Studies of Calcium Phosphate Coatings by FTIR/ATR Techniques. *J. Biomed. Mater. Res.* **1994**, *28*, 1337−1346.
(35) Kong, J.; Yu, S. Fourier Transform Infrared Spectroscopic Analysis of Protein Secondary Structures. *Acta Biochim. Biophys. Sin.* **2007**, *39*, 549−559.
(36) Dzwolak, W.; Kato, M.; Taniguchi, Y. Fourier Transform Infrared Spectroscopy in High-Pressure Studies on Proteins. *Biochim. Biophys. Acta* **2002**, *1595*, 131−144.
(37) Glassford, S. E.; Byrne, B.; Kazarian, S. G. Recent Applications of ATR FTIR Apectroscopy and Imaging to Proteins. *Biochim. Biophys. Acta* **2013**, *1834*, 2849−2858.
(38) Surewicz, W. K.; Mantsch, H. H. New Insight into Protein Secondary Structure from Resolution-Enhanced Infrared Spectra. *Biochim. Biophys. Acta* **1988**, *952*, 115−130.
(39) Dong, A.; Randolph, T. W.; Carpenter, J. F. Entrapping Intermediates of Thermal Aggregation in Alpha-Helical Proteins with Low Concentration of Guanidine Hydrochloride. *J. Biol. Chem.* **2000**, *275*, 27689−27693.
(40) Haris, P. I.; Severcan, F. FTIR Spectroscopic Characterization of Protein Structure in Aqueous and Non-Aqueous Media. *J. Mol. Catal. B: Enzym.* **1999**, *7*, 207−221.
(41) Miller, L. M.; Bourassa, M. W.; Smith, R. J. FTIR Spectroscopic Imaging of Protein Aggregation in Living Cells. *Biochim. Biophys. Acta* **2013**, *1828*, 2339−2346.
(42) Serro, A. P.; Gispert, M. P.; Martins, M. C.; Brogueira, P.; Colaco, R.; Saramago, B. Adsorption of Albumin on Prosthetic Materials: Implication for Tribological Behavior. *J. Biomed. Mater. Res., Part A* **2006**, *78*, 581−589.
(43) Vanea, E.; Tamasan, M.; Albon, C.; Simon, V. Synthesis and Characterisation of a New Composite Aluminosilicate Bioceramic. *J. Non-Cryst. Solids* **2011**, *357*, 3791−3796.
(44) Pourzal, R.; Theissmann, R.; Williams, S.; Gleising, B.; Fisher, J.; Fischer, A. Subsurface Changes of a MoM Hip Implant below Different Contact Zones. *J. Mech. Behav. Biomed. Mater.* **2009**, *2*, 186−191.
(45) Wang, Y. X.; Wang, L. P.; Xue, Q. J. Improvement in the Tribological Performances of Si_3N_4, SiC and WC by Graphite-like Carbon Films under Dry and Water-Lubricated Sliding Conditions. *Surf. Coat. Technol.* **2011**, *205*, 2770−2777.
(46) Hang, R. Q.; Qi, Y. A Study of Biotribological Behavior of DLC Coatings and Its Influence to Human Serum Albumin. *Diamond Relat. Mater.* **2010**, *19*, 62−66.
(47) Wang, J. Z.; Yan, F. Y.; Xue, Q. J. Tribological Behavior of PTFE Sliding against Steel in Sea Water. *Wear* **2009**, *267*, 1634−1641.
(48) Zhang, M.; Wang, X. B.; Fu, X. S.; Xia, Y. Q. Performance and Anti-Wear Mechanism of $CaCO_3$ Nanoparticles as a Green Additive in Poly-alpha-olefin. *Tribol. Int.* **2009**, *42*, 1029−1039.
(49) Park, S. J.; Lee, K. R.; Ko, D. H. Tribochemical Reaction of Hydrogenated Diamond-like Carbon Films: A Clue to Understand the Environmental Dependence. *Tribol. Int.* **2004**, *37*, 913−921.
(50) Mishina, H.; Kojima, M. Changes in Human Serum Albumin on Arthroplasty Frictional Surfaces. *Wear* **2008**, *265*, 655−663.
(51) Mathew, M. T.; Jacobs, J. J.; Wimmer, M. A. Wear-Corrosion Synergism in A CoCrMo Hip Bearing Alloy Is Influenced by Proteins. *Clin. Orthop. Relat. Res.* **2012**, *470*, 3109−3117.
(52) Wang, S. B.; Ge, S. R.; Norm, G.; Michael, V.; Xiao, J. Comparison of the Wear Behavior of UHMWPE Lubricated by Human Plasma and Brine. *J. China Univ. Min. Technol. (Engl. Ed.)* **2007**, *17*, 0335−0340.
(53) Scholes, S. C.; Unsworth, A. The Effects of Proteins on the Friction and Lubrication of Artificial Joints. *Proc. Inst. Mech. Eng. H* **2006**, *220*, 687−693.
(54) Zhang, H. Y.; Luo, J. B.; Zhou, M.; Zhang, Y.; Huang, Y. L. Biotribological Properties at the Stem−Cement Interface Lubricated with Different Media. *J. Mech. Behav. Biomed. Mater.* **2013**, *20*, 209−216.

DOI: 10.1021/am507850r
ACS Appl. Mater. Interfaces 2015, 7, 2772−2783

(55) Wu, W. J.; Pai, T. M.; Hon, M. H. Wear Behavior of Silicon-Containing Diamond-Like Carbon Coatings. *Diamond Relat. Mater.* **1998**, *7*, 1478−1484.
(56) Cui, J. F.; Qiang, L.; Zhang, B.; Ling, X.; Yang, T.; Zhang, J. Y. Mechanical and Tribological Properties of Ti−DLC Films with Different Ti Content by Magnetron Sputtering Technique. *Appl. Surf. Sci.* **2012**, *258*, 5025−5030.
(57) Manninen, N. K.; Ribeiro, F.; Escudeiro, A.; Polcar, T.; Carvalho, S.; Cavaleiro, A. Influence of Ag Content on Mechanical and Tribological Behavior of DLC Coatings. *Surf. Coat. Technol.* **2013**, *232*, 440−446.

DOI: 10.1021/am507850r
ACS Appl. Mater. Interfaces 2015, 7, 2772−2783